Constraint and exploitation of redundant degrees of freedom during walking

Jun Nishii[a,1,*], Yoshimitsu Hashizume[a], Shoko Kaichida[a], Hiromichi Suenaga[a], Yoshiko Tanaka[b]

[a] *Yamaguchi University, 1677-1 Yoshida, Yamaguchi, 753-8512, JAPAN*
[b] *Mitsubishi Electric Information Network Corporation, 1-4-4, Koji-machi, Chiyoda-ku, Tokyo, 102-8483, JAPAN*

Abstract

What kind of leg trajectories are selected during human walking? To address this question, we have analyzed leg trajectories from two points of view: constraint and exploitation of redundant degrees of freedom. First, we computed the optimal leg swing trajectories for forward and backward walking that minimize energy cost for the condition of having some stretch of elastic components at the beginning of the leg swing and found that the optimal trajectories explain the characteristics of measured trajectories. Second, we analyzed how and when leg joints cooperate to adjust the toe position relative to the hip position during walking and found that joint coordination (i.e., joint synergy) is exploited at some control points during human walking, e.g., the toe height when it passes through its lowest position from the ground and the leg posture at the beginning of the double-support phase. These results suggest that the basic constraint in selecting a leg trajectory would be the minimization of energy cost; however, the joint trajectory is not strictly controlled over the entire trajectory and redundant degrees of freedom are exploited to adjust the foot position at some critical points that stabilizing walking.

Keywords: joint synergy, energetic optimality, biped walking, backward walking, uncontrolled manifold analysis

*Corresponding author
Email address: nishii@sci.yamaguhci-u.ac.jp (Jun Nishii)
[1]Tel & Fax: +81 (83) 933 5691

1. Introduction

Redundant degrees of freedom (DOFs) in our bodies are sources of adaptability and dexterity because the redundancy allows for a variety of solutions to accomplish a task. In this paper, we consider the following two problems to understand the underlying control mechanisms that manipulate redundancy during human walking: (1) how the redundancy is constrained and (2) how it is exploited. The first is a traditional problem that asks what kinds of criteria are adopted in the selection of a trajectory from an infinite number of possibilities that can accomplish a given task. This question also asks what the goal of learning is for living bodies, a question that is also important for understanding the learning mechanism of living bodies. The latter is a problem well described in a story told by Bernstein "a skilled blacksmith's hammer hits a given target correctly, but his joint trajectories are not constant and show variability across a series of strikes". From this observation, Bernstein concluded that the variance of each joint trajectory is not independent and that to accomplish a task, variance at critical points (in this case, the hammer position) is suppressed by joint coordination that exploits redundancies [1]. What, then, are the critical points used for stable walking, and how are redundant degrees of freedom in our leg joints exploited during walking? The following sections detail our results concerning these two problems. Section 2 discusses a result about the constraint on DOFs in the selection of leg swing trajectories during forward and backward walking, and section 3 shows analytical results on joint coordination (i.e., joint synergy) during walking.

2. Constraint on redundant degrees of freedom

Many experimental and theoretical studies have reported that locomotor parameters, such as stride length and frequency, are optimized based on energy cost [2, 3, 4, 5, 6, 7]. However, the choice of leg swing trajectory during walking is still under debate. Some work has suggested that no energy supply might be necessary for leg swing [8]; however, some recent studies have suggested that electromyography (EMG) activities are observed during the swing, especially at the end [9, 10].

In previous studies, we computed the optimal leg swing trajectory that minimizes energy cost in a smooth touch-down condition [11, 12]. The results suggested that the optimal trajectory takes a similar form to the measured

one; however, in the latter, the foot was raised slightly higher, which requires additional energy cost in an amount that is explained by the release of elastic energy stored in tendons, which was ignored in previous studies [12].

In this study, we investigated the energetic optimality of the leg swing trajectory for forward and backward walking. For this purpose, we computed the optimal leg swing trajectories that connect the initial and end leg position of the swing phase obtained using human data, considering the effect of elastic components and comparing them with human data.

2.1. Experimental methods

2.1.1. Experimental measurements

We measured the leg swing trajectories of subjects equipped with reflective markers at the hip, knee, ankle and toe while they walked forward and backward on a treadmill at speeds of 4.0 km/h. The subjects were two males in their twenties with no disorder in their lower extremities and gave their informed consent prior to the experiment. The walking speed were not informed to the subjects during the experiment and the measurements were started without notifying them after some period to allow for adaptation to walking on the treadmill. The trajectories were recorded by a motion capture system (Himawari SP200, LIBRARY, Inc.) at 200 fps and smoothed by a 6th-order low-pass Butterworth filter with a cutoff frequency of 6 Hz.

2.1.2. Computation of the optimal trajectory

In the computation of the optimal leg swing trajectories, a leg was modeled as a three-link system with joints at the hip, knee and ankle that move in a 2-dimensional plane (Fig. 1). The trunk was assumed to move horizontally at a constant speed without vertical movement. The length of each link was determined by the body parameters of the subjects. The mass, position of the center of mass and inertia moment of each link were estimated from the weight and link length of each subject by the method described in Winter [13]. The damping coefficients at each joint were referenced from Hatze [14] and Weiss et al. [15]. The details on the body parameters are shown in Appendix A.

As elastic components, the tendon of the iliopsoas muscles and the Achilles tendon were considered (Fig. 1). In the human body, the iliopsoas connects the thigh or pelvis and backbone by curving around the hip joint; however, to simplify the computation, we assumed that the iliopsoas connects the thigh and the front of the hip. The elastic components were modeled as simple

linear springs that do not produce an extension force as actual tendons do not. The elastic coefficients were set to 1.0×10^5 N/m by referring to the data in [16], which indicates that the elastic coefficient of the Achilles tendon is in the range of 1.0×10^5 N/m to 1.0×10^6 N/m. The extension of the tendon at the hip joint at the beginning of swing was assumed to be 15 mm in forward walking and that of the Achilles tendon was assumed to be 1 mm in backward walking. The extension of the Achilles tendon was not considered in forward walking, because the data in Fukunaga et al. [17] suggest that the gastrocnemius medialis tendon shows only negative or small amounts of stretch during the swing phase. The stretch of the tendon at the hip joint in backward walking was also ignored.

In the computation of the optimal trajectory, a sequential quadratic programming (SQP) library, the SNOPT (Stanford Business Software, Inc.) was used and the optimal joint torques at twelve sample points $\tau_i(t_j)$, $(t_j = j/(11T), j = 0, \ldots, 11)$ were computed, where T is the duration of swing phase and subscripts $i = 1, 2, 3$ represent the hip, knee and ankle joint, respectively. The twelve sample points were interpolated using a spline function on torque data every 0.005s, and joint trajectories were computed by an open source software program, Open Dynamics Engine (ODE), from the interpolated torque. The value function to be minimized was the total estimated energy cost E:

$$E = \int_0^T \sum_{i=1}^{3} P(\tau_i(t), \omega_i(t))dt, \tag{1}$$

where ω_i shows the joint angular velocity and P is a function that estimates metabolic rate. In this paper, we used the equation that Alexander proposed based on physiological data [18] as the function P. The joint angles and angular velocities at the toe-off and touch-down positions were randomly selected from typical stride data from the subjects and used as the initial and terminal conditions in the computation (see Appendix A). The swing duration was also given by the data. The Lagrangian and its derivatives required for the computation of the SQP were numerically estimated by a quasi-Newton approximation by the SNOPT.

2.2. Results and discussion

Fig. 2 shows the experimental results. In each figure the origin is set at the hip position. Fig. 2 (a) shows the measured trajectory, and (b) and

(c) show the optimal trajectories not including and including the tendon for forward walking, respectively. In the measured trajectory, the ankle and foot are raised up slightly after toe-off, then fall along a slightly curved line and are retracted before landing. The optimal swing trajectory takes a lower trajectory (Fig. 2(b)) than the actual one (Fig. 2(a)) when no tendon is considered. However, when the initial stretch of the tendon around the hip joint was considered, it lifted up the foot and brought the knee forward, and the optimal trajectory took a shape similar to the actual trajectory (Fig. 2(c)). These results suggest that the swing trajectory during forward walking would be designed to suppress the energy cost and the elastic components would also play a role in the design of the trajectory.

Fig. 2 (d) shows the measured trajectory, and (e) and (f) show the optimal ones not including and including the tendon for backward walking, respectively. In the case of backward walking, we found the quasi-optimal trajectory, in other words, the second best solution, in which the energy cost is slightly higher than for the optimal trajectory. When the tendon was ignored, the energy costs of the optimal and quasi-optimal trajectories were 3.07 J and 3.13 J, respectively, with the former taking a higher trajectory than the actual one and the latter taking a lower trajectory (Fig. 2 (d), (e)). When a slight stretch of the Achilles tendon at the beginning of the swing was considered, the foot in the quasi-optimal trajectory was raised and better matched the characteristics of real human walking (Fig. 2(d)(f)). In this case, the energy costs for the optimal and quasi-optimal trajectories were 3.03 J and 3.33 J, respectively. The reason why the quasi-optimal, as opposed to the optimal, trajectory took a shape similar to the actual trajectory is not known. Our results, however, indicate that backward walking is not simply a matter of reversing the motions of forward walking as suggested by Grasso et al. [19], and like forward walking, it would also be designed to suppress the energy cost. Although in Fig. 2 we showed results given by a subject, we also confirmed that the same results were obtained qualitatively for the other subject.

In running, it is often suggested that the elastic energy stored during stance phase works to reduce the energy cost [20]. Our results suggest that even for walking such elastic energy might be utilized for saving the energy cost required to raise the foot in the middle of swing to avoid stumbling.

3. Exploitation of redundant degrees of freedom

Even for skilled tasks, human movements show variance between trials, as do leg trajectories between strides during walking. However, if the leg swing trajectory is designed to raise the foot in the middle of swing to avoid stumbling, as proposed in the previous section, the variance of the toe height around these points should be bounded in some range. To examine this hypothesis and explore other critical control points for walking, we analyzed the variance of leg trajectories using the Uncontrolled Manifold (UCM) method proposed by Scholz and Schöner [21].

The UCM is defined as a manifold of task variables, such as joint angles, by which a given task is accomplished (Fig. 3). For instance, to set the toe position relative to the hip position at a specific height, there are redundancies in the choice of the angles of the hip, knee and ankle joints. If the variance of the joint angles is bounded around the UCM and is not distributed into its orthogonal direction, we can say that there is joint coordination that suppresses the variance of the toe height, i.e., the redundancy is exploited in the control of the toe height. In this study, we analyzed the degree of the coordination among three leg joints, often called joint synergy, by the UCM method.

3.1. Experimental methods

3.1.1. Measurement of human walking

The subjects were four females in their twenties with no disorder in their lower extremities. We measured the leg trajectories of the subjects, who were equipped with reflective markers at the hip, knee, ankle and toe and walked on a treadmill at 4.5 km/h. The experimental settings are the same as those in section 2.1.

3.1.2. UCM analysis

In this study, we modeled the leg as a simple three-link system that moves in a vertical plane (Fig. 4) and analyzed the leg movement during walking as follows.

The stance and swing phase of the leg trajectory data of 25 strides for each subject were normalized by the duration of each phase, and the average $\bar{\boldsymbol{\theta}}(t) = \left(\bar{\theta}_1(t), \bar{\theta}_2(t), \bar{\theta}_3(t)\right)^T$ of the normalized data was computed for each subject, where t is the normalized time, $\bar{\theta}_i$ $(i = 1, 2, 3)$ shows the averaged joint angle, and the subscript $i = 1$, 2, and 3 represent the hip, knee and

ankle, respectively. The distribution of the deviation of the joint angles $\boldsymbol{\sigma}^k(t) = \boldsymbol{\theta}^k(t) - \bar{\boldsymbol{\theta}}(t)$ was then analyzed by the UCM method, where $\boldsymbol{\theta}^k(t) = \left(\theta_1^k(t), \theta_2^k(t), \theta_3^k(t)\right)^T$ $(k = 1, 2, \ldots, 25)$ is the joint trajectory of the k-th stride (Fig. 3). In the UCM analysis, we selected the joint angles as task variables and the toe height and horizontal toe position relative to the hip position as the performance variables. The analytical method is almost the same as that used in [22]. We summarize the method for the case where we select the UCM as the manifold in the joint angle space on which the toe height is the constant value $y(\bar{\boldsymbol{\theta}})$.

The height of the toe y is a function of the joint angles:

$$y = l_1 \cos\theta_1 + l_2 \cos\theta_2 + l_3 \cos\theta_3, \tag{2}$$

where l_i $(i = 1, 2, 3)$ shows the link length (Fig. 4). In this case, the UCM on which the toe height takes a constant value is two-dimensional and $\boldsymbol{\epsilon}_y^{\perp} = \nabla_{\boldsymbol{\theta}} y|_{\boldsymbol{\theta}=\bar{\boldsymbol{\theta}}(t)}$ shows the orthogonal direction to the UCM at $\boldsymbol{\theta} = \bar{\boldsymbol{\theta}}(t)$. The UCM component $\boldsymbol{\sigma}_y^{k\parallel}(t)$ of the deviation of the k-th stride and its orthogonal component $\boldsymbol{\sigma}_y^{k\perp}(t)$ are given by

$$\begin{cases} \boldsymbol{\sigma}_y^{k\parallel}(t) & = \boldsymbol{\sigma}^k(t) - \boldsymbol{\sigma}_y^{k\perp}(t) \\ \boldsymbol{\sigma}_y^{k\perp}(t) & = (\boldsymbol{\sigma}^k(t) \cdot \hat{\boldsymbol{\epsilon}}_y^{\perp}(t))\hat{\boldsymbol{\epsilon}}_y^{\perp}(t), \end{cases} \tag{3}$$

where $\hat{\boldsymbol{\epsilon}}_y^{\perp}(t) = \boldsymbol{\epsilon}_y^{\perp}(t)/|\boldsymbol{\epsilon}_y^{\perp}(t)|$. We define here two kinds of variances per DOF, one is the UCM component of variance $\sigma_y^{\parallel}(t)$ and the other is its orthogonal component $\sigma_y^{\perp}(t)$ given by

$$\begin{cases} \sigma_y^{\parallel}(t) & = \dfrac{1}{N}\displaystyle\sum_{k=1}^{N} |\boldsymbol{\sigma}_y^{k\parallel}(t)| \\ \sigma_y^{\perp}(t) & = \dfrac{1}{N}\displaystyle\sum_{k=1}^{N} |\boldsymbol{\sigma}_y^{k\perp}(t)|, \end{cases} \tag{4}$$

respectively, where $N = 25$ is the stride number. When $\sigma_y^{\parallel}(t)$ is larger than $\sigma_y^{\perp}(t)$, such a distribution of the joint angles suggests that there is joint synergy that suppresses the deviation of the toe height relative to the hip position. To judge the existence of joint coordination, we defined the degree of synergy S_y by

$$S_y(t) = \frac{\sigma_y^{\parallel}(t)}{\sigma_y^{\perp}(t)}. \tag{5}$$

By the definition, $S_y > 1$ indicates the existence of joint synergy.

In this study, we computed two kinds of UCM components, $\sigma_x^{\parallel}$ and $\sigma_y^{\parallel}$, for the UCMs that do not change the horizontal and vertical components of the toe position, respectively. Their orthogonal components, $\sigma_x^{\perp}$ and $\sigma_y^{\perp}$, and the degrees of synergy, S_x and S_y, were also computed.

3.2. Results and discussion

Fig. 5 shows the UCM components of the variance of the leg joint angles and degree of joint synergy that suppresses the variance of the horizontal and vertical toe position relative to the hip position. Over the entire stride period, $S_y(t)$ is larger than 1 (Fig. 5(b)), which means that the variance of the toe height is suppressed by joint synergy. S_y takes especially high value in the middle of the swing phase (around 85% of the stride time). At that moment, in the middle of the swing phase, the toe passes its lowest position from the ground, which suggests that the variance of the toe height is effectively suppressed by joint synergy, which contributes to avoid accidental stumbling due to fluctuations in leg movement.

Just before the start of the double-support phase, S_y of the stance leg becomes large (around 50% of stride time), which indicates that the variance of the hip height is suppressed by joint synergy for the touch down of the contralateral leg. The variances of the contralateral leg at the moment are shown in around 100% of stride time and all the variances, $\sigma_x^{\parallel}$, $\sigma_x^{\perp}$, $\sigma_y^{\parallel}$, and $\sigma_y^{\perp}$, decrease just before touch-down (Fig. 5(a)(b)), which shows that the variance of the leg posture is suppressed in the end of leg swing.

At the end of the double-support phase (around 60% of stride time), a high value of S_x is observed (Fig. 5(a)). The variances of the contralateral leg at the moment are shown around 10% of stride time and all the variances, $\sigma_x^{\parallel}$, $\sigma_x^{\perp}$, $\sigma_y^{\parallel}$, and $\sigma_y^{\perp}$, take small values (Fig. 5(a)(b)), which shows that the variance of the leg posture is also suppressed at the end of the first double support phase.

The results of this study have shown some control points for human walking. The first is the control of the toe height when it passes its lowest position. Joint synergy that exploits redundant DOFs is utilized at the moment when the risk of stumbling is high. The second is the control of the posture at the start of the double-support phase. At the moment, the hip height is controlled by joint synergy and the variance of the leg posture of the swing leg is suppressed. Some studies in the field of robotics have reported that

the foot position at touch-down is an important factor to enable biped locomotion [23, 24]. Our results suggest that the foot height at the moment of touch-down is adjusted by the cooperation of both legs in human walking. The third is the control of the leg posture at the end of the double-support phase. At the moment the variance of the posture of the leg in the beginning of stance phase is small and the horizontal toe position of the other leg is adjusted by joint synergy. In other words, the horizontal toe position at kick-off phase is adjusted by the cooperation of both legs.

4. Conclusion

The results in this study on the constraint in the selection of the leg trajectory during walking correspond to the swing phase; however, the results and many previous studies discussing the relation between energy cost and locomotor parameters would support the hypothesis that the basic strategy to determine a locomotor pattern is to minimize the energy cost. The results of our analyses have also suggested that the control strategy for walking would not be to make the entire joint trajectory approach the optimal one but to adjust the foot position at some critical points that stabilize walking by exploiting redundant DOFs. For instance, the toe height when it passes through its lowest position from the ground is precisely tuned by joint synergy, which would contribute to the avoidance of stumbling. This finding is also consistent with the result obtained in section 2, which suggests that elastic components contribute to the rising of the foot during leg swing. Just before the beginning of the double-support phase, the hip height is controlled by joint synergy and the variance of the posture of the swing leg decreased, which would suppress the variance of the impact at touch-down and effectively avoid falling down. The UCM analysis also showed that joint synergy is exploited to adjust the horizontal toe position at kick-off phase as well. These findings tell us that joint synergy is utilized at some critical points to produce stable walking, providing a new perspective for understanding the control strategy of human walking.

Our study also includes some limitations that should be considered in future studies. For instance, in the analysis of the constraint in the selection of the leg swing trajectory, we assumed the extensions of the tendon in the iliopsoas for forward walking and the Achilles tendon for backward walking. However, because few studies have measured the length of tendons during walking, we have no physiological data that support our assumptions. In the

analysis of the exploitation of redundancies, we analyzed the leg trajectory in terms of two kinds of UCMs, the horizontal and vertical toe position relative to the hip joint. However, there would be many other possible UCMs to find control points for walking. For instance, the toe velocity could be a potential candidate for examination, because Wisse (2006) suggested that the velocity control of the foot just before touch-down improves the stability of walking [10]. It would also be interesting to consider how such forms of joint synergy are realized, in other words, whether these forms of synergies are controlled by the nervous system or intrinsically embodied in the physical structure of our bodies.

Acknowledgement

This work has been partially supported by a Grant-in-Aid for Scientific Research on Priority Areas "Emergence of Adaptive Motor Function through Interaction between Body, Brain and Environment" from the Japanese Ministry of Education, Culture, Sports, Science and Technology.

Appendix A. Body parameters and boundary conditions in the computation of the optimal leg swing trajectory

The body parameters used in the computation of the optimal trajectory were as follows. The body mass was $M = 63.8$ [kg]; the lengths of the thigh, leg, and foot were $l_1 = 0.49, l_2 = 0.38$ and $l_3 = 0.12$ [m], respectively. The damping coefficients at the hip, knee, and ankle joints were 3.75, 1.05, and 0.44 [kg·m^2/s], respectively.

The joint angles and angular velocities at lift-off and touch-down were $(\theta_1(0),\ \theta_2(0),\ \theta_3(0)) = (-0.129, -0.758, 0.609)$ [rad], $(\dot{\theta}_1(0),\ \dot{\theta}_2(0),\ \dot{\theta}_3(0)) = (2.507, -4.276, -1.266)$ [rad/s], $(\theta_1(T), \theta_2(T), \theta_3(T)) = (0.308, -0.055, 1.129)$ [rad], and $(\dot{\theta}_1(T),\ \dot{\theta}_2(T),\ \dot{\theta}_3(T)) = (-0.657, -2.217, -2.389)$ [rad/s] for forward walking, where $T = 0.480$ [s] is the swing duration. For backward walking, $(\theta_1(0),\ \theta_2(0),\ \theta_3(0)) = (0.385, -0.091, 1.221)$ [rad], $(\dot{\theta}_1(0),\ \dot{\theta}_2(0),\ \dot{\theta}_3(0))(-0.009, 1.397, -3.593)$ [rad/s], $(\theta_1(T), \theta_2(T), \theta_3(T)) = (0.090, -0.997, 1.235)$ [rad], $(\dot{\theta}_1(T),\ \dot{\theta}_2(T),\ \dot{\theta}_3(T))(-3.097, 6.272, 5.027)$ [rad/s], and $T = 0.390$ [s].

References

[1] M. L. Latash, J. P. Scholz, G. Schöner, Toward a new theory of motor synergies, Motor Control 11 (2007) 276–308.

[2] M. Y. Zarrugh, F. N. Todd, H. J. Ralston, Optimization of energy expenditure during level walking, Europ. J Appl Physiol. 33 (1974) 293–306.

[3] M. Y. Zarrugh, C. W. Radcliffe, Predicting metabolic cost of level walking, Europ J Appl Physiol 38 (1978) 215–223.

[4] A. E. Minetti, R. M. Alexander, A theory of metabolic costs for bipedal gaits, J Theor Biol 186 (1997) 467–476.

[5] J. Nishii, Legged insects select the optimal locomotor pattern based on energetic cost, Biol Cybern 83 (2000) 435–442.

[6] J. M. Donelan, R. Kram, A. D. Kuo, Mechanical and metabolic determinants of the preferred step width in human walking, Proc Roy Soc, Lond B 268 (2001) 1985–1992.

[7] J. Nishii, An analytical estimation of the energy cost for legged locomotion, J Theor Biol 238 (2006) 636–645.

[8] S. Mochon, T. A. McMahon, Ballistic walking, J Biomech 13 (1980) 49–57.

[9] A. Seyfarth, H. Geyer, H. Herr, Swing-leg retraction: a simple control model for stable running, J Exp Biol 206 (2003) 2547–2555.

[10] M. Wisse, C. G. Atkeson, D. K. Kloimwieder, Dynamic stability of a simple biped walking system with swing leg retraction, Lecture Notes in Control and Information Sciences 340 (2006) 427–443.

[11] J. Nishii, M. Nakamura, A determinant of the leg swing trajectory during walking, Proc of 3rd Int Symp on Adaptive Motion in Animals and Machines (AMAM) (2005) CD–ROM.

[12] A. Fujii, H. Suenaga, Y. Hashizume, J. Nishii, Variability of leg swing trajectories and their optimality, Proc of 4th Int Symp on Adaptive Motion in Animals and Machines (AMAM) (2008) 173–174.

[13] D. A. Winter, Biomechanics and motor control of human movement, John Wiley & Sons, 3rd edition, 2004.

[14] H. Hatze, A new method for the simultaneous measurement of the moment of inertia, the damping coefficient and the locomotion of the center of mass of a body segment, Europ J Appl Physiol 34 (1975) 217–226.

[15] P. L. Weiss, R. E. Kearney, I. W. Hunter, Position dependence of ankle joint dynamics-I. Passive mechanics, J Biomech 19 (1986) 727–735.

[16] R. Riener, T. Edrich, Identification of passive elastic joint moments in the lower extremities, J Biomech 32 (1999) 539–544.

[17] T. Fukunaga, K. Kubo, Y. Kawakami, S. Fukashiro, H. Kanehisa, C. N. Maganaris, In vivo behaviour of human muscle tendon during walking., Proceedings of the Royal Society B: Biological Sciences 268 (2001) 229–233.

[18] R. M. Alexander, A minimum energy cost hypothesis for human arm trajectories, Biol Cybern 76 (1997) 97–105.

[19] R. Grasso, L. Bianchi, F. Lacquaniti, Motor patterns for human gait: Backward versus forward locomotion, J Neurophysiol 80 (1998) 1868–1885.

[20] R. Blickhan, R. J. Full, Similarity in multilegged locomotion: Bouncing like a monopole, J Comp Physiol A 173 (1993) 509–517.

[21] J. P. Scholz, G. Schöner, The uncontrolled manifold concept: Identifying control variables for a functional task, Exp Brain Res 126 (1999) 289–306.

[22] J. F. Yang, J. P. Scholz, M. L. Latash, The role of kinematic redundancy in adaptation of reaching, Exp Brain Res 176 (2007) 54–69.

[23] H. Miura, I. Shimoyama, Dynamical walk of biped locomotion, Int. J. Robotics Research 3 (1984) 60–74.

[24] M. A. Townsend, Biped gait stabilization via foot placement, J Biomech 18 (1985) 21–38.

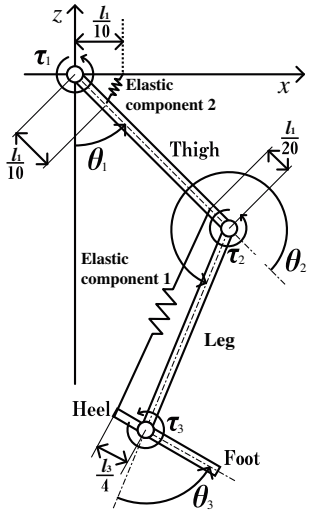

Figure 1: Three-link model of a leg. l_1, l_2, and l_3 are the lengths of the thigh, leg, and foot, respectively.

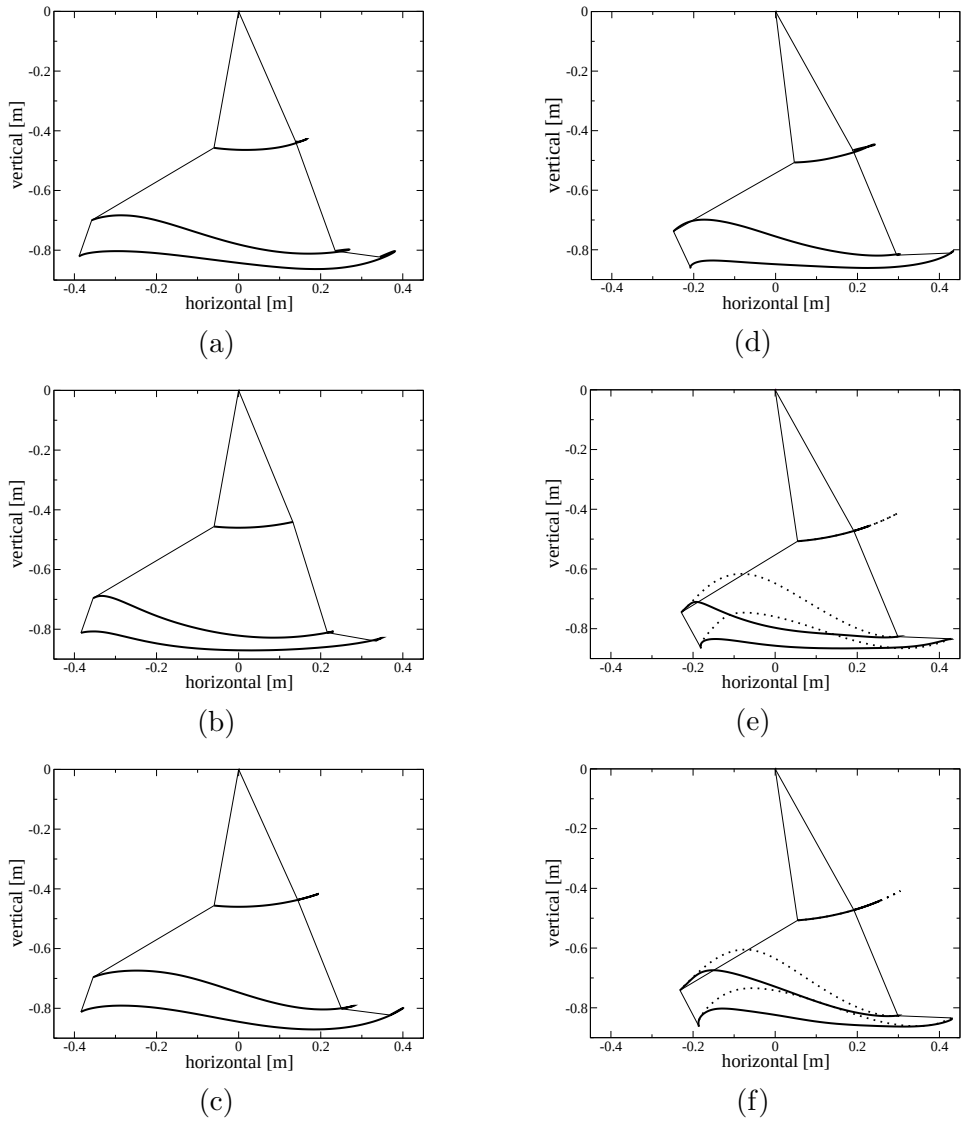

Figure 2: Horizontal view of the measured and optimal leg swing trajectories for forward and backward walking. The left and right figures show the trajectories of forward and backward walking, respectively. The upper figures, (a) and (d), show the measured trajectories. The middle figures, (b) and (e), and the lower figures, (c) and (f), show the optimal trajectories minimizing energy cost not including and including the effect of elastic components, respectively. In each figure, the origin is set at the hip joint, and the upper, middle, and lower lines show the trajectories of knee, ankle, and toe, respectively. In (e) and (f) the optimal (dotted line) and quasi-optimal trajectories (solid line) are shown for backward walking. The lines that connect the hip, knee, ankle, and toe show the leg posture at the start and end of leg swing. The right side of the figure is the walking direction in forward walking and vice versa in backward walking.

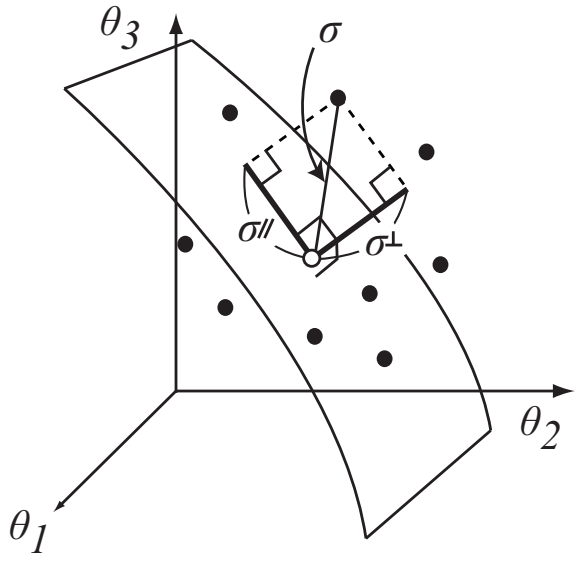

Figure 3: Analysis of variance from the view point of the UCM. The axes show joint angles, the closed circles show the joint angles at a specific stride time during walking, the open circle shows the average of the joint angle data, and the curved surface is the schematic view of the UCM that shows the joint angles needed to realize the same toe height. $\sigma^{\parallel}$ and $\sigma^{\perp}$ show the parallel and orthogonal components of the deviation to the UCM, respectively. The former deviation does not affect the toe position but the latter does.

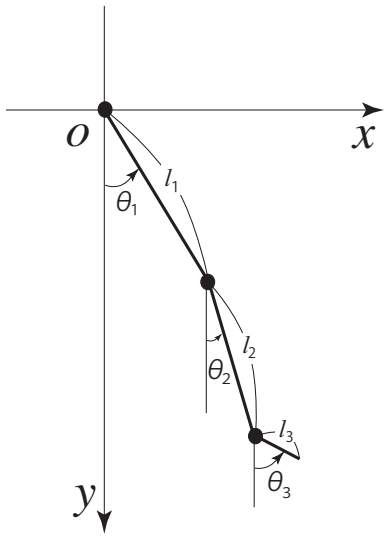

Figure 4: The definition of joint angles in the UCM analysis.

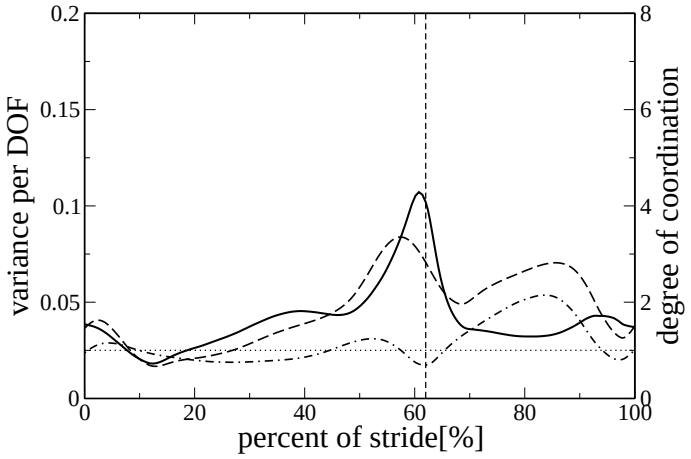

(a)

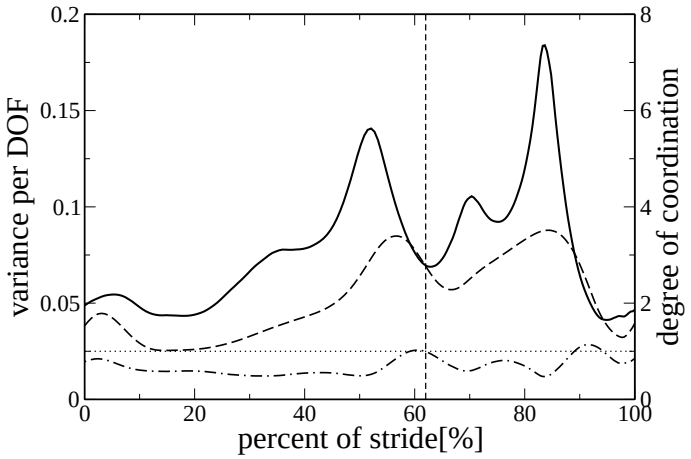

(b)

Figure 5: The degree of joint synergy and variances per DOF during walking. (a) and (b) are the results when the UCMs are assumed to be the manifolds on which the horizontal and vertical toe position are the constants, $\bar{x}(t)$ and $\bar{y}(t)$, respectively. The solid, broken and chain lines show the degree of synergy S_x, $\sigma_x^{\parallel}$, and $\sigma_x^{\perp}$, respectively, in (a), and they show S_y, $\sigma_y^{\parallel}$, and $\sigma_y^{\perp}$, respectively, in (b). The data are the average of the results of the UCM analysis of four subjects. The stride time 0 % shows the beginning of the stance and the time 62% shows the beginning of the swing, where the value 62 % is the average ratio of a stance duration to a stride period.